Authors' Response to the Reviewer Comments

Manuscript title: Critical Role of Dust Induced Electrostatic Coagulation in the Evolution of Aerosol Size Distributions in the Atmosphere

Journal: Atmospheric Chemistry and Physics

Manuscript ID: egusphere-2026-486

Response to Reviewer 1's comments:

This paper aims to address a critical gap in atmospheric aerosol modeling by investigating how electrostatic forces influence coagulation processes of dust particles. The authors applied DMA–APS to retrieve joint size-charge distributions of dust aerosols, which can potentially overcome the lack of single-particle charge measurements. By incorporating aerosol charge into the coagulation kernel, their simulations reveal significant electrostatic effects on particle size distribution. Although the topic of paper is interesting, I have doubts on the methodology used in this work, which need to be cleared before a second round of review.

1. The first critical point is the inherent limitations of the DMA–APS setup. The DMA can only select a finite range of particle mobilities, which makes it impossible to select particles with large sizes and only a few charges, as they their mobility is below the selection limit of the DMA. Therefore, the charge measurements are biased towards higher charge state. Such bias challenges the validity of the measurements and must be addressed in the revision.

Response: Thank you for this important comment. We think this limitation is indeed there but may not be significant for the dust aerosols in the micrometer size range relevant to this study. The mean charge level for the dust aerosols is on the order of 10^2 e, so these aerosols would generally not fall below the lower DMA mobility selection limit under the present operating conditions. According to the electrical mobility definition equation (Eq. (1)), the lower DMA mobility selection limit used in this study was 4.68×10^{-9} $m^2 \cdot V^{-1} \cdot s^{-1}$, which corresponds to a minimum required charge of only ~5 e for an aerosol diameter of ~1 μm, ~10 e for ~2 μm, and ~35 e even near the upper end of the measured size range (~7 μm). Importantly, ~59% of the total dust aerosol number concentration is distributed within the 1 – 2 μm size range, where the lower DMA mobility boundary corresponds to only ~5 – 10 e. However, the mean charge level of dust aerosols in this dominant 1 – 2 μm size range is still on the order of 10^2 e, much higher than the lower-boundary charge values.

$$n = \frac{3\pi\mu D_p Z_p}{eC} \quad (1)$$

Z_p is the electrical mobility ($m^2 \cdot V^{-1} \cdot s^{-1}$), n is the number of charges per particle, e is the elementary charge (1.6×10^{-19} C), π is the circular constant, and μ is the dynamic viscosity of air (1.85×10^{-5} Pa·s at 25 °C), D_p is the electrical mobility diameter (m), C is the

Cunningham slip correction factor (*Seinfeld, J. H., & Pandis, S. N. Atmospheric Chemistry and Physics: From Air Pollution to Climate Change. 3rd ed. John Wiley & Sons, 2016*).

C is calculated as:

$$C = 1 + \frac{2\lambda}{D}[1.257 + 0.4\exp(-\frac{1.1D}{2\lambda})] \quad (2)$$

D is the aerosol diameter (m), λ is the molecular mean free path (68×10^{-9} m).

The number fraction of dust aerosols outside the lower DMA mobility limit was estimated on a particle size bin basis. For each particle size bin, the charge value corresponding to the lower DMA mobility boundary was first calculated based on Eq. (1). The number concentration below this boundary was then supplemented based on the fitted charge distribution for that particle size bin. Specifically, the charge distribution in each particle size bin was empirically fitted using a Gaussian-shaped function in ln(n) space:

$$N_{D_p}(n)=A_{D_p}exp[-\frac{(ln\ n-\mu_{D_p})^2}{2\sigma_{D_p}^2}] \quad (3)$$

where n is the number of charges per particle, D_p is the particle diameter of a given size bin, $N_{D_p}(n)$ is the number concentration at charge state n for particles with diameter D_p, and A_{D_p}, μ_{D_p}, and σ_{D_p} are empirical fitting parameters obtained separately for each particle size bin.

Therefore, under the present DMA operating conditions, only **~0.6%** of the dust aerosols in this study are estimated to fall below the lower DMA mobility limit.

In addition, even if the undetected dust aerosol fractions were large, it is also unlikely to substantially affect the results of this study. The contribution of these large weakly charged aerosols to electrostatic coagulation enhancement is expected to be limited. Our measurements show that dust aerosols can exhibit charge distributions significantly higher than those predicted by the Boltzmann charge equilibrium distribution. Such bipolar high-charge characteristics imply a faster electrostatic coagulation rate among dust aerosols (*Adachi et al., Electrostatic coagulation of bipolarly charged aerosol particles, Journal of Chemical Engineering of Japan, 14, 467 – 473, https://doi.org/10.1252/JCEJ.14.467, 1981*). In contrast, large weakly charged aerosols, with charge levels close to or even lower than those expected under Boltzmann charge equilibrium, are expected to exhibit a much weaker electrostatic coagulation effect.

Furthermore, aerosols with zero charge are explicitly included in the size-charge distribution in this study. Therefore, the potential bias caused by incomplete coverage of low-charge aerosols is not further amplified in the modeling.

Changes to the manuscript:

Lines 157-178: In addition, the finite DMA mobility selection range may introduce a small

bias toward higher inferred charge states for large aerosols. This is because aerosols with large diameters and only a few charges may fall below the lower DMA mobility selection limit and therefore cannot be fully selected. According to the electrical mobility definition equation, the lower DMA mobility selection limit used in this study, 4.68×10^{-9} $m^2 \cdot V^{-1} \cdot s^{-1}$, corresponds to a minimum required charge of only ~5 e for aerosols with diameters of ~1 μm, ~10 e for ~2 μm, and ~35 e even near the upper end of the measured size range (~7 μm). Importantly, ~59% of the total dust aerosol number concentration is distributed within the 1 – 2 μm size range, where the lower DMA mobility boundary corresponds to only ~5 – 10 e. However, the mean charge level of dust aerosols in this dominant 1 – 2 μm size range is still on the order of 10^2 e, much higher than the lower-boundary charge values.

The number fraction of dust aerosols outside the lower DMA mobility limit was estimated on a particle size bin basis. For each particle size bin, the charge value corresponding to the lower DMA mobility boundary was first calculated based on the electrical mobility definition equation. The number concentration below this boundary was then estimated from the fitted charge distribution for that particle size bin. Specifically, the charge distribution in each particle size bin was empirically fitted using a Gaussian-shaped function in ln(n) space:

$$N_{D_p}(n)=A_{D_p} exp[-\frac{(ln\ n-\mu_{D_p})^2}{2\sigma_{D_p}^2}]$$

where n is the number of charges per particle, D_p is the particle diameter of a given size bin, $N_{D_p}(n)$ is the number concentration at charge state n for particles with diameter D_p, and A_{D_p}, μ_{D_p}, and σ_{D_p} are empirical fitting parameters obtained separately for each particle size bin. Based on this particle size bin based estimation, only ~0.6% of the dust aerosols in this study are estimated to fall below the lower DMA mobility limit. Therefore, under the present operating conditions, the dust aerosols considered in this study would generally remain above the lower DMA mobility selection limit.

2. For quantitative assessment of the previous point, please add particle size to Table S2 assuming the particle only carries 1 charge. Also, please add the information of DMA sheath flow rate.

Response: Thank you for this constructive suggestion. We have added to Table S2 the aerosol diameters corresponding to the prescribed electrical mobility under the assumption of a single elementary charge (1e). In addition, we have added the DMA sheath flow rate used for number of charges per particle measurements of dust aerosols, which was 10 LPM.

Changes to the manuscript:

Lines 114-117: The laboratory-generated dust aerosols were then directed into the Differential Mobility Analyzer (DMA, Models 3080 and 3082, TSI Inc., inlet flow rate: 1 LPM, sheath flow rate: 10 LPM) at prescribed electrical mobilities Z_p (Table S2), and the aerodynamic diameter of the classified aerosols was measured with an APS.

Changes to the supplement:

Lines 117-119:

Table S2. DMA operating electrical mobility Z_p set points for selecting dust aerosols with specific electrical mobilities.

No.	Z_p ($m^2 \cdot V^{-1} \cdot s^{-1}$)	Correspondent aerosol diameter at Z_p for a single charge (1e) (μm)	Charge number below which 5% of particles fall	Correspondent diameter at 5% charge (μm)	Median charge number	Correspondent diameter at median charge (μm)	Charge number below which 95% of particles fall	Correspondent diameter at 95% charge (μm)
1	4.68×10^{-9}	0.197	4	0.784	9	1.765	32	6.275
2	7.83×10^{-9}	0.118	5	0.586	16	1.875	56	6.563
3	1.36×10^{-8}	0.068	11	0.742	26	1.754	101	6.815
4	2.48×10^{-8}	0.037	19	0.703	50	1.85	178	6.586
5	4.64×10^{-8}	0.02	37	0.732	91	1.8	334	6.605
6	8.95×10^{-8}	0.01	70	0.718	186	1.907	657	6.736
7	1.76×10^{-7}	0.005	135	0.704	340	1.773	874	4.557
8	3.51×10^{-7}	0.003	299	0.782	567	1.482	932	2.437
9	7.03×10^{-7}	0.001	563	0.735	725	0.946	957	1.249

3. The second critical point is that dust particles produced by the dust aerosol generators are representative only of the freshly produced dust particles. After some time in the atmospheres, I would expect their charge state are significantly reduced (as shown in the simulations). Please make this point very clear in the manuscript.

Response: Thank you for this important comment. We agree with the reviewer that the aerosols generated by the dust aerosol generator are representative of newly generated or near-source dust aerosols. To avoid over-extrapolation, we have added corresponding clarifications in the revised manuscript.

Changes to the manuscript:

Lines 102-103: It should be noted that these aerosols are more representative of freshly generated dust aerosols under near-source conditions than of aged atmospheric dust after

long-range transport.

Lines 334 – 342: The dust aerosols used in this study are more representative of freshly generated dust aerosols. As coagulation and related processes proceed during atmospheric transport, the charge states of dust aerosols are generally expected to decrease. Therefore, the PSD evolution trend shown here is more representative of dust source regions and near-source conditions. However, in real atmospheric transport, dust plumes may continuously mix with newly emitted or entrained aerosols that retain relatively high initial charges. Such continuous input could delay charge decay and sustain stronger electrostatic coagulation over a longer timescale, thereby affecting the timescale of PSD evolution. The above discussion suggests that the transition from freshly generated, highly charged dust to more aged and weakly charged dust during atmospheric transport deserves more explicit consideration in future modeling studies.

4. Is mass conservation checked for the simulation model? It seems that the product particle is put into a single bin rather than distributed between neighboring bins, which is common practice in aerosol simulations with the sectional method (the distribution method is well documented in the literature).

Response: Thank you for this valuable comment. We checked the mass conservation. The mechanism of mass loss in the current model is as follows. The mass loss mainly arises from the numerical discretization error introduced when continuously calculated coagulation products are mapped to a single discrete size bin in the current sectional coagulation model. Specifically, when the equivalent volume diameter of a coagulation product does not yet exceed the boundary of the next size interval, the product cannot be partially allocated to the larger bin according to its continuous position. This introduces errors in mass and volume. Even with finer size discretization, this error caused by mapping from a continuous to a discrete representation remains difficult to eliminate completely. It becomes more pronounced in coagulation cases with large aerosol-size differences, such as coagulation between dust aerosols and ambient sub-500 nm aerosols. For example, when a 1.085 μm dust aerosol coagulates with a 21.7 nm ambient sub-500 nm aerosol, the equivalent-volume diameter of the product is

$$D_{new}=(1.085^3+0.0217^3)^{1/3}\approx 1.085003\ \mu m$$

Since the next larger size bin in the present bin setting is 1.166 μm, this new diameter is still too small to enter the next bin. Therefore, the coagulation product remains assigned to the original 1.085 μm bin in the current sectional model. Accordingly, this error mainly affects the quantitative characterization of the rightward shift of the dust aerosol PSD after coagulation. For clarity, Figure R1 illustrates the mass loss during coagulation induced by size bin discretization.

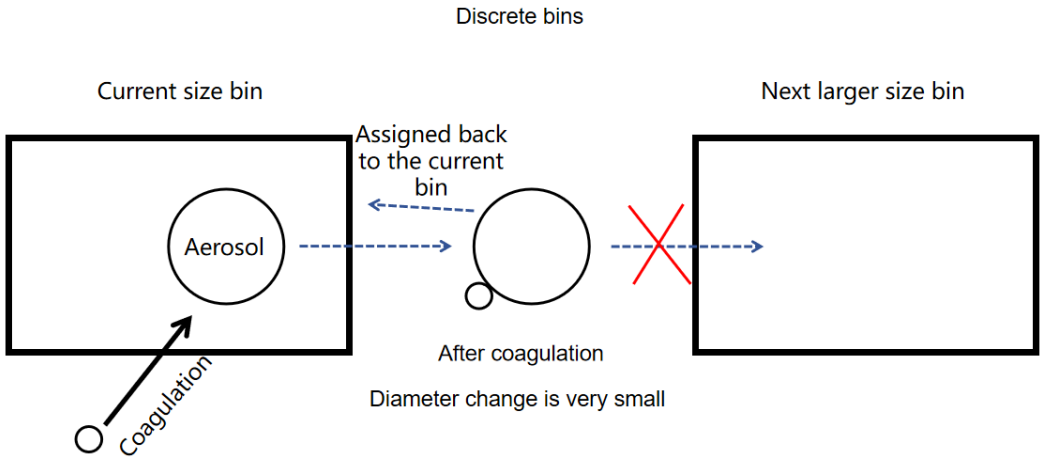

Figure R1. Schematic illustration of a coagulation product remaining in the current size bin.

On this basis, we note that the above mass loss has only a limited influence on the differences in PSD evolution between the two coagulation mechanisms. Specifically, this mass loss mainly occurs during the rightward shift of the dust aerosol PSD after coagulation. Assuming constant aerosol density and using the cubic relationship between mass and aerosol diameter, the above ~10 – 20% mass difference corresponds to an underestimation of the rightward shift of the dust aerosol PSD by ~3% – 7%. This is clearly smaller than the magnitude of the differences in PSD evolution caused by the two coagulation mechanisms in this study.

Changes to the manuscript:

Lines 383 – 398: It should be noted that, in the mixed aerosol system, the numerical mass loss is more pronounced for coagulation between dust aerosols and ambient sub-500 nm aerosols because of their large size difference. This mass loss mainly arises from the representation of a physically continuous increase in aerosol volume, and thus equivalent diameter, using discrete size bins in the sectional coagulation model. When a dust aerosol coagulates with a much smaller ambient sub-500 nm aerosol, the equivalent-volume diameter of the coagulation product may increase only slightly and may still remain within the original dust aerosol size bin rather than entering the next larger bin. For example, when a 1.085 μm dust aerosol coagulates with a 21.7 nm ambient sub-500 nm aerosol, the equivalent-volume diameter of the coagulation product is only approximately 1.085003 μm, which is still below the next larger size bin of 1.166 μm. Therefore, the coagulation product remains assigned to the original 1.085 μm dust aerosol size bin, and the small increase in aerosol volume is not fully reflected as a rightward shift of the dust aerosol PSD. Assuming constant aerosol density and the cubic relationship between aerosol mass and aerosol diameter, a ~10 – 20% mass loss corresponds to only a ~3% – 7% equivalent-diameter difference because aerosol mass scales with the cube of aerosol diameter. Thus, this numerical uncertainty mainly affects the quantitative magnitude of the dust aerosol PSD shift, but is unlikely to alter the qualitative differences in PSD evolution between Brownian coagulation and electrostatic coagulation in the mixed aerosol system.

5. Please elaborate on the method to compile figure 3 from DMA–APS measurements. My understanding is that each DMA–APS measurement at a fixed DMA voltage provide an oblique

line in the mobility diameter-charge space, how are the raw data inverted to give dN/dlogdp?

Response: The reviewer's understanding is correct that each DMA–APS measurement at a fixed DMA voltage (i.e., under a prescribed electrical mobility condition) corresponds to one oblique line in the size–charge space, as determined according to Eq. (1). The number of charges per particle n in Eq. (1) was determined from the prescribed electrical mobility Z_p and the aerodynamic diameter D_a, which was then converted to the electrical mobility diameter D_p using Eq. (2). Under each prescribed electrical mobility condition, the APS provided the dN/dlogD_p values for the DMA-classified dust aerosols over a series of logarithmically spaced particle-diameter bins, i.e., bins with equal intervals in logD_p. For each logarithmic particle-diameter bin under each prescribed electrical mobility condition, the corresponding number of charges per particle n was then calculated from Eq. (1) using the prescribed electrical mobility Z_p and the converted electrical mobility diameter D_p. For simplicity, no joint concentration normalization was applied over the particle-size and charge dimensions. The concentration was expressed as dN/dlogD_p, not as a combined two-dimensional form such as dN/(dlogD_p dn) or dN/(dlogD_p dlog$n$). Each dN/dlogD_p value was assigned to the corresponding calculated charge number n. The size–charge distribution was reconstructed from multiple DMA–APS measurement lines obtained under different prescribed electrical mobility conditions. The bins not directly covered by these measured lines were then filled by linear interpolation of aerosol number concentration between adjacent lines to reconstruct the full two-dimensional distribution.

$$n = \frac{3\pi\mu D_p Z_p}{eC} \tag{1}$$

Z_p is the electrical mobility ($m^2 \cdot V^{-1} \cdot s^{-1}$), n is the number of charges per particle, e is the elementary charge (1.6×10^{-19} C), π is the circular constant, and μ is the dynamic viscosity of air (1.85×10^{-5} Pa·s at 25 °C), D_p is the electrical mobility diameter (m), C is the Cunningham slip correction factor (*Seinfeld, J. H., & Pandis, S. N. Atmospheric Chemistry and Physics: From Air Pollution to Climate Change. 3rd ed. John Wiley & Sons, 2016*).

$$D_p = D_a \sqrt{\chi^3 \frac{\rho_0 C(D_m)^2 C(D_a)}{\rho_p C(D_{ve})^3}} \tag{2}$$

is derived from the following two equations:

$$\frac{D_p}{C(D_p)} = \frac{D_{ve}\chi}{C(D_{ve})} \tag{3}$$

$$D_a = D_{ve} \sqrt{\frac{\rho_p C(D_{ve})}{\chi \rho_0 C(D_a)}} \tag{4}$$

χ is the dynamic shape factor under the experimental conditions (set to 1.0 assuming spherical dust aerosols), D_a is the aerodynamic diameter (m), D_{ve} is the volume equivalent diameter (m), ρ_0 is the reference density (1 g/cm^3), and ρ_p is the density of dust aerosol particles, taken as 2.65 g/cm^3.

Changes to the manuscript:

Lines 132 – 144: Under each prescribed electrical mobility condition Z_p, the APS provided the PSD (dN/dlogD_p) of the DMA-classified dust aerosols for different aerodynamic diameter bins. The aerodynamic diameter D_a measured by the APS was converted to the electrical mobility diameter D_p using Eq. (3). For each logarithmic particle-diameter bin （logD_p bin）, the corresponding number of charges per particle n was then calculated from Eq. (1) using the prescribed Z_p and the converted D_p. Therefore, each prescribed electrical mobility condition produced one aerosol number concentration line in the two-dimensional size-charge space.

For simplicity, the concentration was not jointly normalized over the particle-size and charge dimensions. It was expressed as dN/dlogD_p, rather than as a combined two-dimensional concentration form such as dN/(dlogD_p dn) or dN/(dlogD_p dlog$n$). Each dN/dlogD_p value was assigned to the corresponding calculated charge number n. The full two-dimensional size-charge distribution was reconstructed from multiple measured lines obtained under different prescribed electrical mobility conditions, and the bins not directly covered by these measured lines were filled by linear interpolation between adjacent lines.